ORIENTAL JOURNAL OF CHEMISTRY
An International Open Access, Peer Reviewed Research Journal
www.orientjchem.org
ISSN: 0970-020 X
CODEN: OJCHEG
2024, Vol. 40, No.(4):
Pg. 920-932

Review of Cerium-based Catalysts and Eco-friendly Oxidants for Chlorine-free Benzaldehyde Production Via Selective Oxidation of Benzyl Alcohol

GANESH BABU BATHULA[1], N. O. GOPAL[2], NARSAIAH CHELIMELA[1], MOHAN KURRA[1], S. SHARAT KUMAR GOUD[1], RAMESHWAR NIMMA[1], SATYANARAYANA MAVURAPU[1], JONNALAGADDA S. B[3]* and CHANDRA SEKHAR VASAM[1]*

[1]Department of Pharmaceutical Chemistry, Telangana University, Nizamabad-503322, India.
[2]Department of Physics, Vikrama Simhapuri University, Nellore-524324, India.
[3]School of Chemistry & Physics, University of KwaZulu-Natal, Durban-4000, South Africa.
*Corresponding author E-mail: csvasamsa@gmail.com

http://dx.doi.org/10.13005/ojc/400402

(Received: June 04, 2024; Accepted: August 07, 2024)

ABSTRACT

This review article describes the designing and aptness of diverse range of cerium-based catalysts for the oxidation of benzyl alcohols (Bz-OLs) in producing exclusively benzaldehydes (Bz-ALs) in the presence of eco-friendly oxidants. The discussion highlights the significance of surface and structural properties inherent to cerium-based catalysts, including the abundance of oxygen vacancies, the redox properties of Ce^{3+}/Ce^{4+} couple, their acid-base characteristics and morphology influence, which play crucial roles in substrate adsorption, reorganization of bonding between substrate and oxidant in promoting selective oxidation reactions. The consolidated data tables (1-4) comprising the best conditions optimized with various ceria based heterogeneous reported so far between the years 2019-2024 is included in the following sections to assess the catalyst design and performance.

Keywords: Cerium-based catalysts, Mixed oxide matrices, Chlorine-free benzaldehyde production, Benzyl alcohol oxidation, Eco-friendly oxidants.

INTRODUCTION

Benzaldehyde (Bz-AL) stands as an industrially significant chemical, particularly as a crucial starting material or intermediary for manufacturing numerous organic compounds across various industries[1]. Currently, the chemical industry employs two main methods for large-scale Bz-AL production: the direct oxidation of toluene or the hydrolysis of benzyl chloride[2-4]. However, both methods are associated with specific challenges, including the formation of unwanted by-products, lengthy processing times, potential catalyst deactivation, high reaction temperatures, and the use of hazardous oxidants such as chromate and potassium permanganate[5,6]. Therefore, considering

the principles of green chemistry, there is a demanding need to advocate for alternative synthetic routes to produce Benzaldehyde[7].

Given the challenges associated with the recovery of traditional oxidants and the separation of products, there has been a notable emphasis on developing catalytic oxidation methods for converting Bz-OL to Bz-AL. This focus is driven by the desire to utilize non-harmful oxidants such as molecular oxygen (O_2), tert-butyl hydroperoxide (TBHP), and hydrogen peroxide (H_2O_2)[8]. To address this objective, numerous researchers have investigated effective and recyclable solid catalysts, including transition/main-group metal oxides, supported metal oxides, mono/mixed metals, zeolites, MOFs, and mesoporous materials. Within this array of heterogeneous catalysts, cerium-based catalysts have garnered significant interest for their utility in the selective oxidation of Bz-OL to Bz-AL[9].

Among the compounds of cerium, the CeO_2 (ceria) exhibits the ability to release and uptake oxygen, a characteristic attributed to its redox nature stemming from the Ce^{3+}/Ce^{4+} ions couple[10,11]. This property facilitates the creation of more reactive oxygen defects, which are crucial for the catalytic oxidation activity of ceria. However, it's noteworthy that at elevated temperatures, ceria is susceptible to sintering, a process that results in the agglomeration of particles that weakens the catalytic performance. Modified ceria catalysts with appropriate isovalent/aliovalent Lewis acidic cations are recommended not only to enhance thermal stability but also to exhibit distinct redox possessions, abundant oxygen vacancies, sufficient acid-base characteristics, smaller crystalline size, and greater definite surface area compared to unmodified ceria[12,13]. A modification in the preparation technique enables the synthesis of modified ceria particles with precise control over the nucleation and growth rates during crystal formation[14]. This crucial characteristic of ceria has been utilized in various applications such as CO oxidation, methane partial oxidation, volatile organic compound oxidation, and the water–gas shift (WGS) reaction, particularly in automotive contexts[15,16].

This review articles focuses the recent trends in the development of different cerium-based catalysts with varied compositions, morphology and surface properties and their efficacy in promoting the selective oxidation of Bz-OL to Bz-AL in high yields. Since we are concerned about recent trends of the above topic, the articles published between the years 2019-2024 were only reviewed. In order to provide a convenient discussion on published literature, the present review is divided in to the following four sections:

1. Ceria supported Noble-metal based catalysts promoted oxidation of Bz-OL to Bz-AL
2. Ceria supported non-Noble-metal based catalysts promoted oxidation of Bz-OL to Bz-AL
3. Unsupported ceria catalysts promoted oxidation of Bz-OL to Bz-AL

Ceria supported Noble-metal based catalysts promoted oxidation of Bz-OL to Bz-AL:

Zheng *et al.,* deduced the connectivity between the morphology (rod, polyhedral, cube, and meso) of ceria supports in Pd/CeO_2 catalysts and their catalytic performance in the aerobic selective oxidation of Bz-OLs[17] (Scheme 1). Physicochemical characteristics were evaluated using XRD, N_2 adsorption-desorption, TEM, XPS, and O_2-TPD methods. They observed varied catalytic activity among Pd catalysts supported on different ceria materials, directly linked to the morphologies of ceria. Notably, Pd supported on polyhedral shaped ceria exhibited the highest catalytic activity. The superior performance of Pd/CeO_2 catalyst comprised of polyhedral shaped ceria was attributed to its higher fraction of Pd^{2+} species, increased Ce^{3+} species and superior O_2-activating capacity as compared to other Pd/CeO_2 materials. This catalyst maintained its activity even after five consecutive uses.

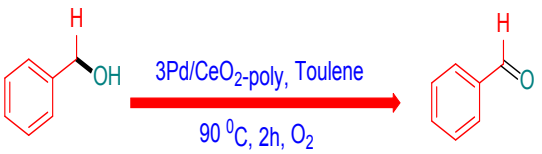

Scheme 1

Ko *et al.,* evaluated the efficiency of three different Pd/CeO_2 nanostructured catalysts in performing a sequential coupling-oxidation on 4-iodobenzyl alcohols[18] (Scheme 2). Impregnation of Pd on ceria and subsequent post-treatment such as calcination and reduction under H_2 atmosphere yielded the (i) Pd single-atom, (ii) Pd nanoclusters and (iii) PdNPs in a sequence on ceria nanorod support. Regarding the catalytic activity, experimental evidences indicate the surface Pd(0) species are

responsible active sites for cross-coupling and Pd-Ceria inter-phases are responsible active site for alcohol oxidation. At this juncture, it was identified that the surface structure of ceria supported Pd-nanoclusters possesses balance between aforementioned two active sites and displayed highest catalytic activity. The details of investigated cross-coupling and simultaneous oxidation processes of alcohols are depicted in Scheme 2.

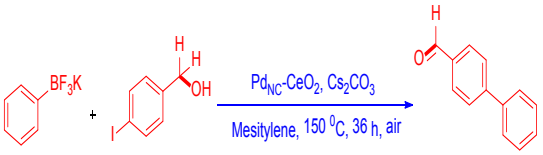

Scheme 2

Zhang *et al.,* reported the role of crystal plane in nano-ceria materials supported palladium catalysts in catalyzing Bz-OL oxidation[19] (Scheme 3). Three nanocatalysts with varied morphologies and crystal planes designated as Pd/CeO_2-rods, Pd/-CeO_2-octahedral and Pd/CeO_2-cubes were tested in this work and observed that the Pd/CeO_2-rods catalyst worked well than others. The surface exposed (110) plane of Pd/CeO_2-rods catalyst was found to advance the oxygen defects and active and supported catalyst interaction thereby to fasten the oxidation catalysis. Substrate scope was also reported in this article.

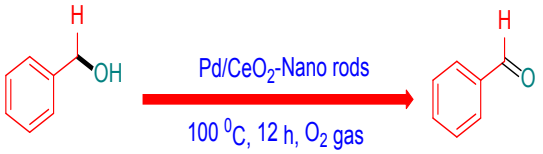

Scheme 3

Moeini and colleagues[20,21] investigated the feasibility of an oxidized-Pd and reduced-Pd impregnated ceria nanorods in oxidizing Bz-OL selectively to Bz-AL in protic and non-protic solvents and under solventless conditions (Scheme 4). The authors noticed that the oxidized-Pd catalyst is highly active in protic solvents and reduced-Pd catalyst was highly active in aprotic solvents for the Bz-OL oxidation, which was ascribed to two different mechanisms. The study also proposed mechanistic theories based on catalytic performance and catalyst analysis, offering a promising avenue for eco-friendly recyclable oxidation of Bz-OL selectively to Bz-AL.

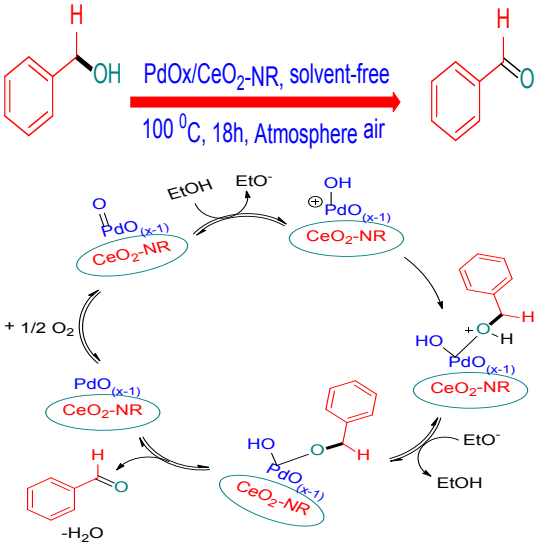

Scheme 4

Wang *et al.,* noted new observations in the reaction mechanism of O_2-mediated Pd/CeO_2 catalyzed solventless oxidation of Bz-OL_{22} (Scheme 5). In addition to the role of metallic (Pd(0)) active centers in oxidation, the role of active oxygen species and Pd (II) species were also recognized by the authors. Atomic layer deposition method was used to prepare this supported catalyst. An appropriate reaction mechanism for alcohol oxidation was proposed in the following scheme 5 to show the participation of both Pd (0)/Pd (II) active centers.

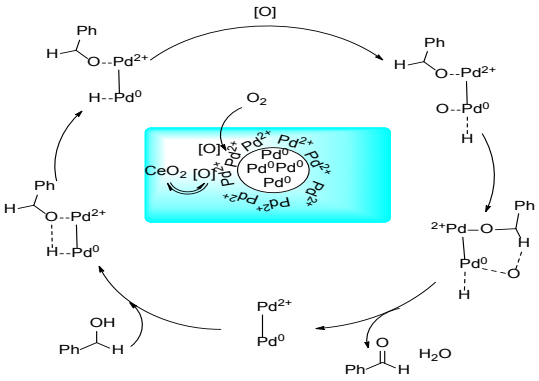

Scheme 5

Yi *et al.,* reported[23] (Scheme 6) about the effectiveness of C_3N_4-CeO_2 supported PdNPs as catalyst in the O_2 mediated oxidative conversion of Bz-OL to Bz-AL under solventless conditions at 90°C. The Pd/C_3N_4-CeO_2 catalyst material was obtained by treating the Pd (II)Cl_2 with C_3N_4-CeO_2 via wet-impregnation followed by reduction with $NaBH_4$. Other materials such as Pd/C_3N_4, C_3N_4-CeO_2

and Pd/CeO_2 were also tested in the oxidation for comparison. It was evident that the catalyst with 3Pd/CN-1.0/CeO_2 composition endowed with best results of Bz-AL selectivity and Bz-OL conversion. This catalyst was recycled successfully six times without any change in the activity in the said oxidation. The accessibility of Pd (0) and Ce (III) active sites on the above catalyst has improved the desired oxidation to produce high yields Bz-AL. A total five benzaldehyde derivatives were synthesized in this work.

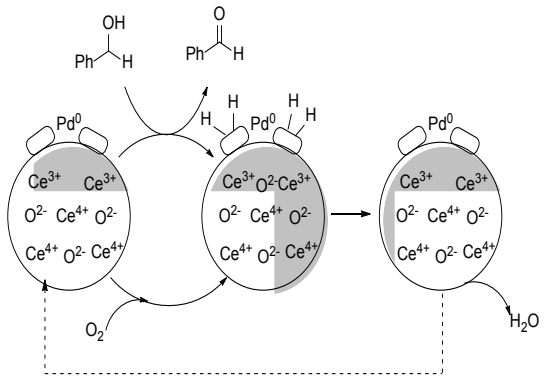

Scheme 6

The report by Feng *et al.,* disclosed that the ceria obtained by the decomposition of cerium nitrate is an effective support to obtain catalytically active Pd/CeO_2 materials in the Bz-OL oxidation under solventless conditions[24] (Scheme 7). A relation between the concentration of oxygen defects and the catalyst activity was explained.

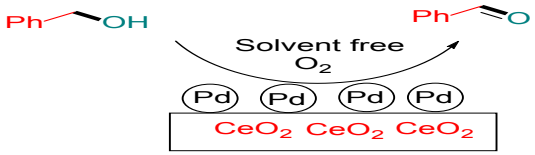

Scheme 7

Wu *et al.,* prepared a polymeric ionic liquid mircrospheres (PILM) protected Pd/CeO_2 nano core-shell structured material. The agglomeration of palladium nanoparticles of this material was found to be influenced by the combination of ceria in the core-shell structure. The PILM/Pd/CeO_2 nanomaterial catalyzed oxidation of Bz-OL[25] (Scheme 8) was optimized by varying the reaction parameters/conditions such as temperature, oxidant and substrate concentration. This catalyst retained the efficacy up to five consecutive cycles. Finally, a plausible reaction mechanism involving the interplay between Pd (II), Ce(IV)/Ce(III), oxide ions in promoting the Bz-OL conversion selectively to Bz-AL was illustrated (Scheme 8).

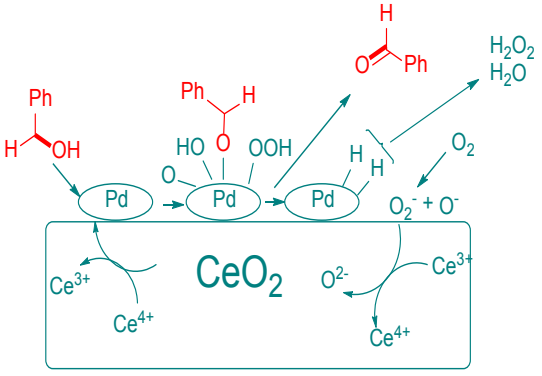

Scheme 8

Wattanakit and colleagues explained the usefulness of nanoceria modified Pt/zeolite catalyst for the oxidation of Bz-OL[26] (Scheme 9). The beneficial effect of each constituent in the composite catalyst in the synergistic oxidation catalysis was systematically analyzed by these researchers. The roles of ceria and zeolite were elucidated. As the concentration of ceria increased, there was improvement in the rate of reaction and desired product selectivity. This article also described the effect of the ratio between Al: Si in the zeolites in tuning the progress of the oxidation. This article also encompasses a suitable reaction mechanism. The authors also provided the catalytic results obtained with other zeolites for comparison and to highlight the usefulness of the present catalyst.

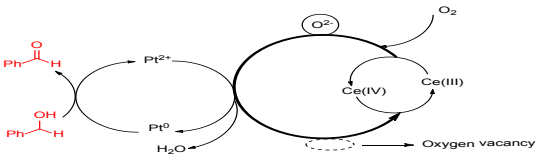

Scheme 9

Hamaloglu and colleagues reported the evaluation of monodisperse-porous CeO_2 microspheres as a potential support system for Palladium nanoparticles (PdNPs) impregnation. These microspheres boast impressive characteristics: they resist aggregation, demonstrate inherent catalytic action, and make easy the retrieval of catalysts post-oxidation[27] (Scheme 10). Moreover, they foster a synergistic interplay with catalytic active centers, such as PdNPs, Ce(III)/Ce(IV) redox couple on the porous surface of the catalyst. Scheme 10 shows a schematic representation elucidating the synergistic interaction between ceria microspheres and PdNPs during the TBHP mediated oxidative conversion of Bz-OL to Bz-AL. The superior catalytic activity of the above material was further supported by computational calculations.

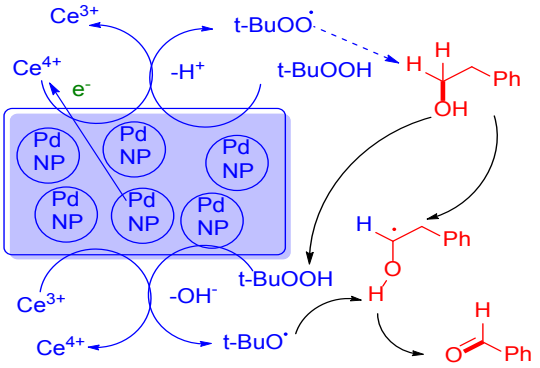

Scheme 10

Lei *et al.,* reported that when air/O_2 is used as an oxidant in the Au/CeO_2 catalyzed conversion of Bz-OL to Bz-AL in toluene at 100°C, the size and type of gold particle dispersion on ceria support influences the catalytic activity[28] (Scheme 11). During the assessment of catalytic properties of three Au species (i) isolated single atoms (Au-SAs), (ii) nanoclusters (Au-NCs), and (iii) nanoparticles (AuNPs) supported on ceria nanorods in Bz-OL oxidation, the Au-SA/CeO_2 catalyst displayed superior activity than the other two catalysts due to the presence of sufficient oxygen vacancies in the interfacial –Ce-O-Au- network. This feature is found to promote the Bz-OL adsorption, its –O-H bond dissociation and removal of β-hydride from alkoxide intermediate by Au(III)/Au(I) couple during the catalytic cycle. DFT calculations were conducted to support the aptness of Au-SA/CeO_2 nanorods catalyst structure and performance in Bz-OL oxidative conversion to Bz-AL. The CeO_2 nanorods were prepared by hydrothermal method. Thereafter, single Au atoms were impregnated by using $HAuCl_4$ as precursor in the presence of $(NH_4)_2CO_3$ via ultrasonic irradiation. Catalyst recycling experiment experiments were also performed in this work. The optimized reactions were extended to study the other alcohols such as n-butanol, cyclohexanol, 2-octanol and n-octanol.

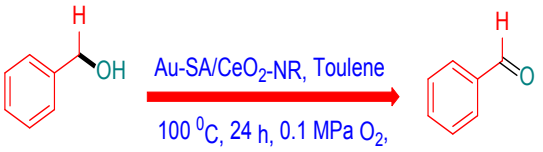

Scheme 11

Table 1: Brief details of Ceria-supported Pd-based catalysts promoted oxidation of Bz-OL to Bz-AL

Sr. No	Optimized catalyst	Catalyst Preparation Method	Oxidant/Solvent	Bz-OL Conversion/Bz-AL yield/selectivityC/Y/S)	Reaction Temperature (°C)	Reference
1	3Pd/CeO_2-polyhedral	Wet-impregnation	O_2/Toluene	93/93/>99	90	17
2	Pd-nanoclusters/CeO_2	Wet-impregnation	Air/Mesitylene	-/63/-	150	18
3	Pd/CeO_2-nanorod (110)	Wet impregnation	O_2 or O_2/Ar/Toluene	75/-/99	90	19
4	PdO_x/CeO_2-nanorods	Wet impregnation	Air/ethanol	93/-/96	78	20
5	PdO_x/CeO_2-NR	Wet impregnation	Air/solventless	50/-/93	100	21
6	20Pd/CeO_2	Deposition	O_2/solventless	90/-/94.5	120	22
7	3Pd/C_3N_4-1.0/CeO_2	Sol-Gel	O_2/solventless	77.2/76.4/>99	90	23
8	Pd@CeO_2	Wet impregnation	O_2/solventless	72.6/70/96.3	90	24
9	PILM/Pd/CeO_2	Wet impregnation	O_2/Water	48/-/98	160	25
10	1Pt/20CeO_2-ZSM-5	Wet impregnation	O_2/Toluene	97.6/100/100	80	26
11	Pd/CeO_2 microspheres	Wet impregnation	TBHP/DEFDME	96.3/93/97	80	27

Li *et al.,* explored the influence of ceria morphology (rods, cubes, and polyhedrons) on the catalytic activity of a supported bimetallic Au-Pd(NPs)/CeO_2 for O_2 mediated Bz-OL oxidation under solvent-free conditions[29] (Scheme 12). They synthesized these different morphologies using the hydrothermal method and employed a deposition-precipitation approach with urea as the precipitating agent to anchor Au-Pd bimetallic NPs onto ceria supports with varied morphologies. Their findings underscored a substantial impact of ceria morphology on the catalytic efficiency of Au-Pd/CeO_2. Specifically, Au-Pd NPs supported on ceria rods displayed superior Bz-OL conversion rates, whereas Au-Pd NPs supported on ceria cubes exhibited the highest selectivity for Bz-AL production. The authors also noticed that the unsupported ceria showed limited catalytic activity in the above conversion. Catalyst characterization techniques revealed that the rod shaped in Au-Pd(NPs)/CeO_2 contains ample number of oxygen defects, Pd(II) and Ce(III) cations on the surface to accelerate the Bz-OL oxidation. This study highlights the crucial role of catalyst support structure in dictating the outcome of Bz-OL oxidation catalysis.

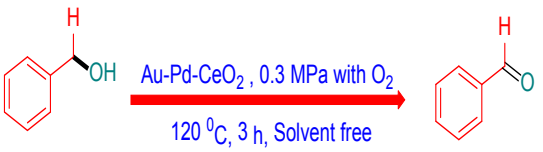

Scheme 12

Wolski *et al.,* explored how co-precipitation agents (hexamethylenetetramine/urea and NaOH) influenced the characteristics and catalytic activity of nano Au-CeO_2 in the oxidation of Bz-OL at RT in water[30] (Scheme 13). The catalyst characterization data revealed that the choice of co-precipitation agent significantly impacted the size and uniformity of AuNPs dispersed on ceria support. Instant co-precipitation with NaOH yielded smaller and more uniform AuNPs compared to gradual co-precipitation with hexamethylenetetramine/urea. The size of AuNPs played a crucial role in enhancing activity in the low-temperature oxidation of Bz-OL. This study offers valuable insights for refining the synthesis of nano Au-CeO_2 catalysts to improve catalytic performance in environmentally friendly alcohol oxidation reactions using molecular oxygen as an oxidant.

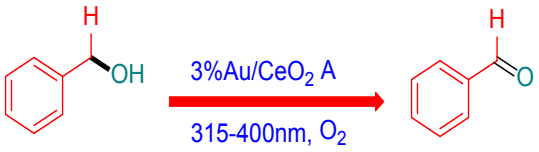

Scheme 13

Lopez *et al.,* explored the utilization of AuNPs supported on ceria as photocatalysts in the selective oxidation of Bz-OL and 4-methoxyBz-OL to the corresponding Bz-ALs under UV, Visible, and natural solar light irradiation. A commercial ceria sample and lab-synthesized ceria were used as supports to immobilize AuNPs with varied concentrations (1 and 3 wt%). No catalytic oxidation was observed using bare ceria. Nevertheless, the AuNP immobilized ceria has shown improved conversion of Bz-OLs and selectivity towards corresponding Bz-ALs specifically under visible and solar light irradiation[31] (Scheme 14). The strong visible light absorption by AuNPs around 565–570nm was attributed to surface Plasmon resonance (SPR), a promoting factor for the conversion of Bz-OL. Moreover, increasing the amount of AuNPs from 1 to 3% further boosted the photocatalytic activity of the above designed catalyst. The synergistic interaction between ceria and AuNPs allowed for efficient utilization of both UV and visible light, leading to enhanced catalytic performance in the said oxidation process.

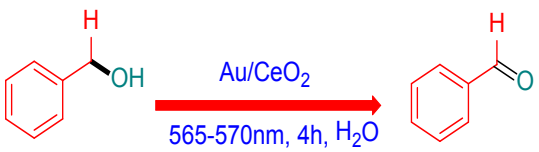

Scheme 14

Chen and colleagues identified the effect of dimension/structure and the ratio between the constituent metals and temperature displayed by Au-PdNPs/CeO_2-ZrO_2 catalyst in the molecular oxygen mediated conversion of Bz-OL to Bz-AL[32] (Scheme 15). Firstly, the authors prepared the above mixed metallic supported catalyst via concurrent deposition–precipitation. Later, it's particle size, structure and composition were modified via oxidation at three different higher temperatures (250, 450 and 700°C). The catalyst calcined at 250°C displayed good catalytic activity than others due to the smaller particle size distribution and the ideal ratio between Au: Pd metallic species. The results of oxidation obtained with pure Au, Pd catalysts and a physical mixture of Au and Pd on a CeO_2-ZrO_2 supported catalyst were used to comparison. The cooperativity between the constituent metals in the designed Au-PdNP/CeO_2-ZrO_2 catalyst is identified in enhancing the oxidation processing.

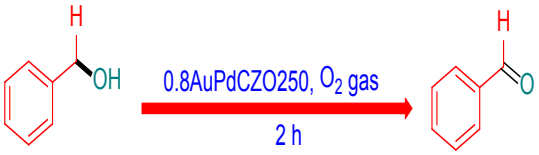

Scheme 15

Liang and colleagues showed that ceria incorporated Au/CNT catalyst performed well than the simple Au/CNT catalyst in the conversion of Bz-OL to Bz-AL due to the creation of surface defects, active oxygen species of CeO_2-lattis and improved synergistic catalysis[33] (Scheme 16). A two step methodology involving colloid immobilization followed by deposition precipitation was implemented to obtain Au-CeO_2/CNT catalyst. This catalyst can be recycled successfully for five times.

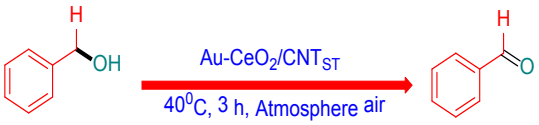

ST= Solvothermal

Scheme 16

Gu *et al.,* described the construction of a hybrid photocatalyst comprising Ag nanoparticles doped CeO_2-shell with Au core via wet-chemical deposition method for the amino Bz-OL oxidation in the presence of molecular oxygen[34](Scheme 17). The incorporation of AgNPs into ceria core-Au shell helped to improve the SPR excitation of Au in the visible to NIR light region, capturing of photons

and thereby accelerated the sequential process of photocatalysis. The photocatalytic mechanism of above conversion was postulated (Scheme 17).

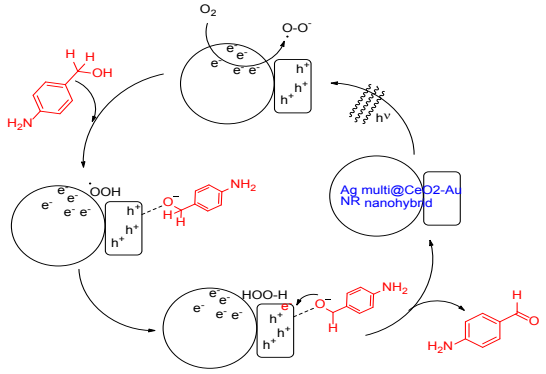

Scheme 17

Chowdhury and colleagues studied the impact of gold on nominal bismuth doped ceria nanomaterials (Au/Bi-CeO_2) on oxygen mobility and lattice defects and its implication in improving the conversion of Bz-OL[35] (Scheme 18). Variations in oxygen defects concentrations and their effect on exposed planes are found to significantly influence the catalytic activity of different ceria shapes (rods, cubes). The ceria surface with gold and bismuth composition was analyzed by various physico-chemical techniques. The influence of bismuth on (110) and (100) exposed planes of gold-ceria nanorods and nanocubes during the catalytic oxidation of Bz-OL were identified. Among these catalysts, Au/Bi-CeO_2 nanorods exhibited the superior activity due to the availability of sufficient number of lattice defects of Frenkel-type. Overall, a good synergism between gold, bismuth and ceria was noticed to optimize the catalytic conditions of said oxidation.

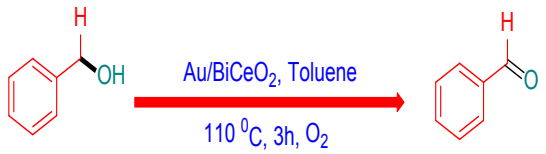

Scheme 18

Aneggi and colleagues investigated the catalytic efficiency of oxidized ruthenium impregnated on ceria-zirconia support matrix in the solventless oxidation of Bz-OL mediated by molecular O_2 at a temperature range of 70-90°C and the monitored the progress of the reaction by proton NMR study[36] (Scheme 19). Regarding the catalyst characteristics, XPS study reveals presence of oxidized ruthenium (RuO_2) on ceria-zirconia surface and formed a Ru-O-Ce linkage, which is crucial to promote the oxidation of Bz-OL. Formation of such linkage enabled the better mobility of oxygen and formation of super oxide ions on cerium sites to support the enhancement in selective catalytic oxidation of Bz-OL to Bz-AL with ~100% selectivity. The authors claimed that above catalyst showed good E-factor<1 that is suitable for sustainable process development.

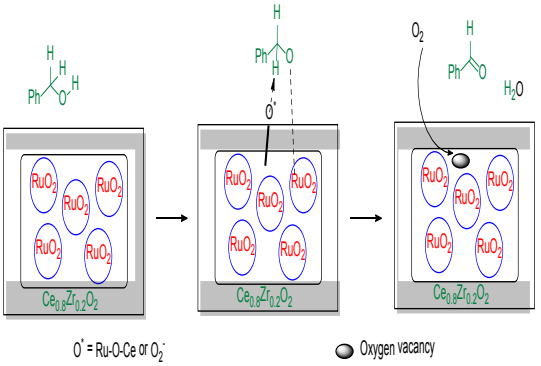

Scheme 19

Laga *et al.,* studied the combined effect of heterogeneous nano-ceria systems and homogenous Ru or Ir-organometallic oxidation catalysts to optimize a redox cooperative catalytic approach for the selective synthesis of Bz-AL in organic solvents in both anaerobic and aerobic catalytic alcohol dehydrogenation processes[37] (Scheme 20). As shown in Scheme-20, the organometallic catalysts dehydrogenate the Bz-OL to Bz-AL and forms an organometallic-H_2 adduct. Now, the nano-ceria acts as terminal oxidant and captures the two hydrogens from organometallic-H_2 adduct. The CeO_2-H_2 adduct is now subjected for oxidation with molecular oxygen to convert back to dehydrogenated form. The authors claimed that this is the first evidence that ceria can oxidize the organometallic hydrides.

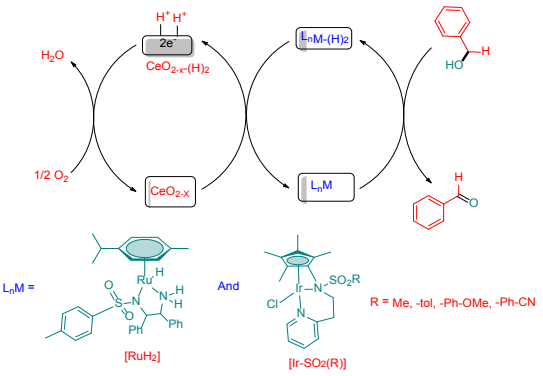

Scheme 20

Table 2: Brief details of Ceria-supported gold-catalysts promoted oxidation of Bz-OL to Bz-AL

Sr. No	Optimized Catalyst	Catalyst Synthesis	Oxidant/Solvent	Bz-OL Conversion Bz-AL Yield/ SelectivityC/Y/S	Reaction Temperature (^{0}C)	Reference
1	Au-SA/CeO_2-nano rods	Hydro thermal/Impregnation	O_2, Ar, or O_2/Ar/Toluene	89/-/94	100	28
2	Au-Pd-CeO_2(cubes)	Deposition-precipitation	O_2/Solvent less	48.84/-/94.33	120	29
3	Au-CeO_2	Co-precipitation with Urea	O_2/Water	17/-/56	40	30
4	3%Au/CeO_2	Deposition-precipitation	Visible radiation 450-560nm-O_2/Water	44/-/95	RT	31
5	0.8Au-Pd/CeO_2ZrO_2	Deposition-precipitation	O_2/cyclo-hexane	90/-/98	80	32
6	Au-CeO_2/CNT	Deposition-precipitation	O_2/p-Xylene	79/-/99	100	33
7	Ag@CeO_2–Au	Wet-chemicaldeposition	O_2–420nm (visible light)/water	>90/-/100	RT	34
8	3.5Au/Bi-CeO_2	Deposition-precipitation	O_2/Toluene	-/-/99	110	35
9	Ru/CeO_2-ZrO_2	Wet-impregnation	O_2/solvent less	61/-/100	70-90	36
10	CeO_2+Ru/Ir-OMCs	Precipitation	Air/Toluene	-/38/-	80	37

Ceria supported non-Noble-metal based catalysts promoted oxidation of Bz-OL to Bz-AL

Volpe and colleagues assessed the performance of copper (5-20%) impregnated ceria catalysts during the aerobic oxidative conversion of Bz-OL to Bz-AL in aqueous medium under refluxing conditions[38] (Scheme 21). The catalysts with high Cu-Ce(III) concentration and low surface acidity performed well in terms of selectivity.

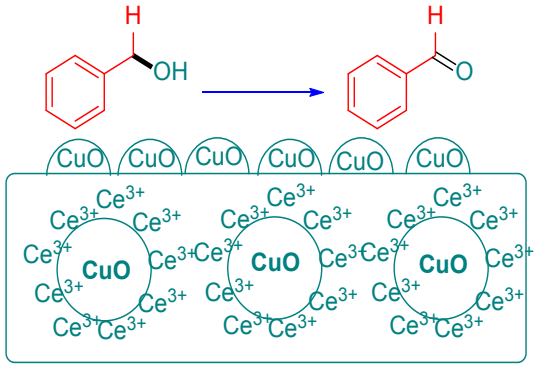

Scheme 21

Pischetola *et al.,* observed the influence of the oxidation copper (0, +1 and +2) during the dehydrogenation of Bz-OL to Bz-AL that was coupled with hydrogenation of phenyl acetylene to styrene/ ethyl benzene[39] (Scheme 22). The coupled processes were more effective than the individual dehydrogenation and hydrogenation. A correlation between Cu^0/Cu^+ on ceria support was observed during dehydrogenation/ hydrogenation was identified with experimental evidence. This article highlights the implication of such coupled process without the need of external hydrogen supply.

Kamaraju and colleagues reported a CO_2 assisted dehydrogenation of Bz-OL to Bz-AL catalyzed by CuNPs supported on cubic shaped ceria[40] (Scheme 23). No external oxidant was used in this work. The existence of weak to strong basic sites in Cu-CeO_2 catalysts was demonstrated by CO_2-TPD findings. The important feature of this study is the role of CO_2 to retain the constant activity of the catalyst in the presence of N_2 carrier gas. As shown in the Scheme 23, the H_2 gas generated in-situ during the oxidation process was suppressed by CO_2 involved water-gas shift reaction. Moreover, there was a mixable compatibility CO_2 and Bz-OL. The activation of Bn-O-H bond was caused by the regulated acid-base sites on the ceria surface, and the α-H of the alcohol –O-H was cleaved by adjacent Cu nanoparticles to produce Bz-AL.

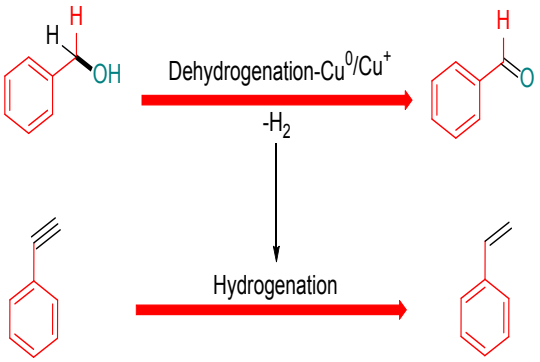

Scheme 22

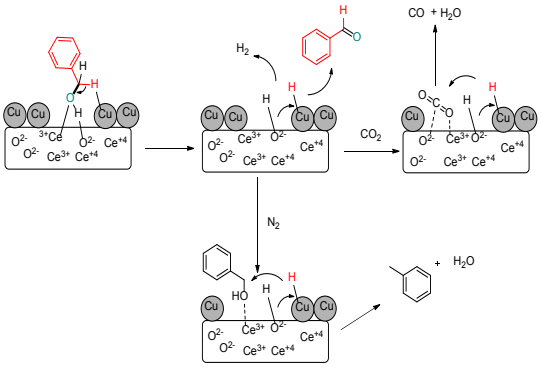

Scheme 23

Han and colleagues designed a nitrogen-doped carbon layers encapsulated ceria nanosheet catalyst with 3D assembly for the efficient conversion of Bz-OL to Bz-AL using atmospheric air as an oxidant[41] (Scheme 24). Firstly, the authors described the design and synthesis of above supported ceria catalyst by metal–organic framework template method and deduced the catalyst surface structure by various characterization techniques. The catalyst surface has shown the availability of sufficient number of active sites for the catalytic oxidation. The key feature of this structure lies in its uniform coating of nitrogen-doped carbon (N–C) layers, which is anticipated to play a crucial role in both the adsorption and activation of benzylic alcohol molecules. The distinct three-dimensional hierarchical arrangement, achieved by the self-assembly of ultrathin nanosheets, offers a plethora of active sites for catalytic reactions and synergism between the ceria and N-C layered structures. Consequently, the CeO_2@N-C USHR demonstrates remarkable catalytic performance in the selective oxidation of benzylic alcohols, particularly in aqueous environments (Scheme 24).

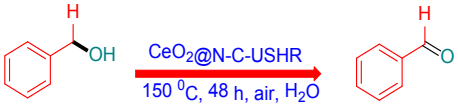

USHR = ultrathin nanosheet self-assembled hierarchical structure

Scheme 24

Density Functional Theory (DFT) calculations provided additional support for the availability of required activities on this catalyst for the selective oxidation of Bz-OL to Bz-AL. The influence of reaction parameters such catalyst dosage and temperature on Bz-OL conversion and catalyst recycling performance were evaluated.

Priya *et al.,* described the designing of a binary CeO_2-SmO_2 impregnated SiO_2 catalyst via wet-impregnation method and its application in the H_2O_2 mediated conversion of Bz-OL to Bz-AL in CH_3CN[42] (Scheme 25). Most interestingly a rise-husk derived SiO_2 is employed as support to impregnate the binary CeO_2-SmO_2 composition. Catalyst characterization techniques disclosed that both CeO_2 and SmO_2 particles are uniformly dispersed on the support. Effect of catalyst loading, solvent and temperature on the reaction was evaluated in optimizing the catalytic conditions. Overall, the supported catalyst with $50CeO_2$-$50SmO_2/SiO_2$ composition was found to exhibit superior catalytic activity in this work. Further, the spent catalyst was activated at 400^0Cand recycled four times successfully without change in the activity.

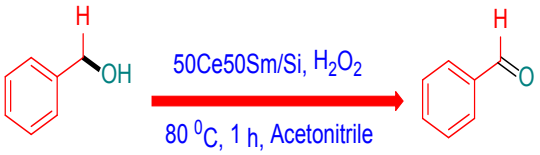

Scheme 25

Manganese-based catalysts have been showing excellent performance in oxidation catalysis. By considering the structural features associated with MnO_2 and CeO_2, Mazumder *et al.,* reported the synthesis and catalytic efficiency of MnOx–CeO_2 binary oxide in the oxidative conversion of Bz-OL to Bz-AL in vapor-phase[43] (Scheme 26). A co-precipitation regime was followed to synthesize these binary oxide catalysts with varied Mn: Ce ratios. Structural analysis revealed the presence of both fluorite-CeO_2 and pure α-MnO_2 phases. Results of catalytic conversion of Bz-OL unveiled that the binary oxides are more efficient than pure MnO_2 and providing support for the concept of synergism in oxidation. It was stated that ceria assists the surface adsorption Bz-OL, while MnO_2 assists the oxidation at the interface. Finally, it is understood that the outstanding oxygen storage capacity of ceria excellent made it an effective support for MnO_2, promoting strong oxygen activation and facilitating Bz-OL oxidation. As depicted in Scheme 26, the ceria phase initiates the substrate adsorption and manganese oxide promotes the oxidation of Bz-OL with its tetravalent Mn(IV) active sites.

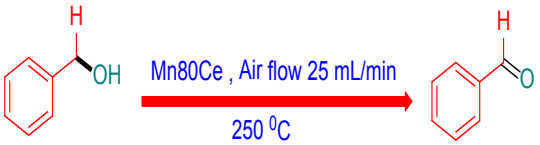

Scheme 26

Turgut *et al.,* described the preparation of iron-borate and ceria mixed metal catalysts (Fe_3BO_6–CeO_2) with varied ceria loadings via ball milling method and used them as catalysts in the H_2O_2 mediated solventless oxidation of Bz-OL to Bz-AL[44] (Scheme 27). The results indicate that 5%

ceria dopant is optimal to optimize the catalytic conditions with appreciable Bz-AL selectivity at 90°C.

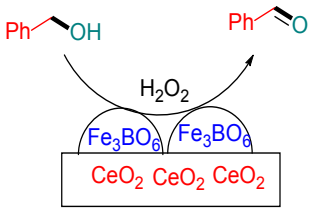

Scheme 27

Xu and colleagues reported the result of the performance some multi-metal oxide catalysts (3d-series) doped with cerium during the solventless oxidation of Bz-OL[45] (Scheme 28) in the presence molecular O_2-oxidant at 150°C. The 3d-series elements combination of Cr-Mn-Fe-Co-Ni with diverse metallic active sites has emerged as new generation catalyst for various heterogeneous catalytic conditions. Stabilization of the entropy of these multi-metal oxide catalysts is the important issue to promote their catalytic activity. A co-precipitation regime can be followed to prepare these doped catalysts. Concerning the results of catalytic oxidation of Bz-OL, the cerium doped catalysts are found to efficient than un-doped catalysts. The presence of cerium altered the structural properties of the catalyst and advanced the oxygen supply mechanism in the catalysis. The authors have also presented a reasonable mechanism that how the doped catalysts involved in the catalytic cycle.

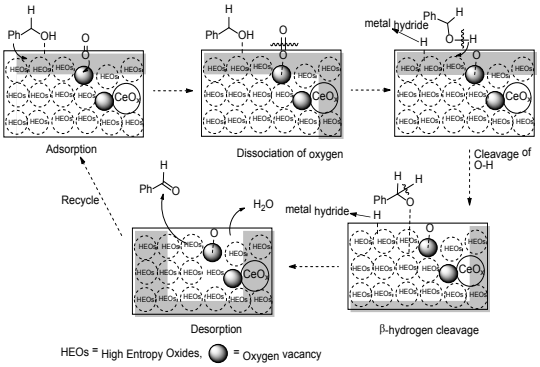

Scheme 28

Aiube and de Macedo examined the influence of cerium metal precursor and the oxidation number of cerium in modifying the properties of Ce-MCM-41 catalysts synthesized for Bz-OL oxidation catalysis. This article mentioned the use of three different cerium salts namely ceric ammonium nitrate $(NH_4)_2[Ce^{+4}(NO_3)_6]$, Cerium Chloride $(Ce^{+3}Cl_3 \bullet 7H_2O)$ and $(Ce^{+3}(NO_3)_3 \bullet 6H_2O)$ to obtain above mixed-material catalysts and designated them as Ce-MCM-CAN (1), Ce-MCM-Cl (2) and Ce-MCM-NO_3 (3), correspondingly. Catalytic oxidation data specify that catalyst (1) exhibited better activity than the other two catalysts in the presence of TBHP oxidant[46] (Scheme 29). The oxidation process by catalysts 2 and 3 was retarded after some times and assigned for the difference in the active sites compared to catalyst 1. According to the characterization data, catalyst (1) possesses both active isomorphous cerium sites and non-framework ceria-NPs that are bound to the surface of MCM-41.

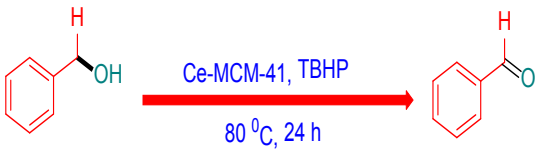

Scheme 29

Meijboom and colleagues elucidated the performance of surface modified mesoporous Ceria-Zirconia mixed oxide catalysts in the TBHP mediated oxidations of Bz-OL[47] (Scheme 30). The mesoporous mixed-oxide catalysts with varied Ce:Zr ratios were prepared by mixing appropriate precursors in 1-butanol in the presence of P-123 polymeric surfactant and water. An inverse micelle was formed by P-123 to modify the surface of catalyst. The $CeZrO_2$ (Ce: Zr = 0.8:0.2) catalyst exhibited good performance than other mixed oxides used in the oxidative conversion of Bz-OL. The performance of above said catalyst was ascribed to the enlarged pores, huge surface area, augmented oxygen defects and surface oxide-ions as active basic-sites. The recyclability of the catalyst is mentioned but the full details were not provided.

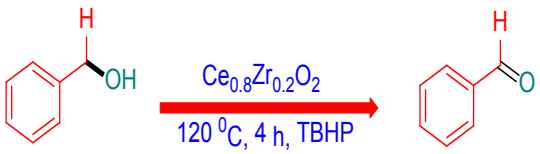

Scheme 30

Table 3: Brief details of ceria supported non-Noble metal catalysts promoted oxidation of Bz-OL to Bz-AL

Sr. No	Catalyst	Catalyst Synthesis	Oxidant / Solvent	Bz-OL Conversion/ Bz-AL Yield/Selectivity C/Y/S	Reaction) Temperature (^{0}C	Reference
1	Cu20-CeO_2	Wet impregnation	O_2/Water	60/-/90	120	38
2	Cu/CeO_2	Deposition-precipitation or standard impregnation	Dehydrogenation/ solventless	-/-/100	160	39
3	20Cu-CeO_2	Co-precipitation	O_2/supercritical CO_2	95.8/-/ 97.7	Ambient	40
4	CeO_2@N–CUSHR	Solvothermal	Air/water	99.9/99.9/100	150	41
5	50Ce50Sm/SiO_2	Wet impregnation	H_2O_2/acetonitrile	55.5/-/ 91.4	80	42
6	$MnO_2$80-CeO_2	Co-precipitation	O_2/solventless	28/-/97	250	43
7	Fe_3BO6-CeO_2	Ball milling	H_2O_2/solventless	34.3/-/81.5	90	44
8	1.0Ce/HEOs(Cr-Mn-Fe-Co-Ni)$_3O_4$	Co-precipitation	O_2 gas & solvent less	31.3/29.3/93.7	150	45
9	CeO_2-MCM-41	Co-precipitation	TBHP/solvent less	54.6/-/47.4	80	46
10	$Ce_{0.8}Zr_{0.2}O_2$	Inverse micelle-based	TBHP/Solvent less	92.53/-/100	120	47

Unsupported-Ceria based catalysts promoted oxidation of Bz-OL to Bz-AL

Fan and colleagues discovered the combined effect of oxygen vacancies and crystal-plane effect of structured ceria nanomaterials (rods, cubes, spherical and octahedron) in accelerating the gas-phase oxidation[48] (Scheme 31) of Bz-OL at 230^{0}C. According to HR-TEM, XPS and TPR data, the ceria catalyst with nonrod morphology possesses higher number of oxygen defects than nanocubes, nano-octahedron and nanoparticles and exhibited high activity in the Bz-OL oxidation. DFT calculations part concerning the catalytic activity indicated that the high catalytic activity of ceria-nonrods is indeed the combined effect of both oxygen vacancies and rod-shape morphology which showed enhanced ability in removing H, adsorbing O_2 and removing H_2O. The catalytic data of this article indicates that there is a relation between the surface structure and morphology of ceria nanomaterials to control the above oxidation.

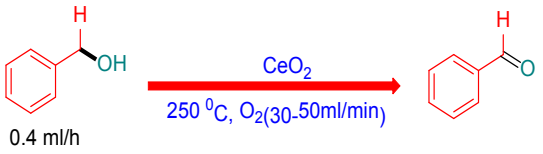

Scheme 31

Cui *et al.,* explored the efficiency of three ceria-based materials as visible light active photocatalysts for the oxidation of Bz-OL to Bz-AL[49] (Scheme 32). The three different ceria-based photocatalysts were prepared by hydrolyzing the Ce-nitrate precursor under three different atmospheres namely oxygen, argon and air, denoted as ceria-O_2, ceria-Ar and ceria-air. The photocatalytic oxidation efficacy of ceria-O_2 was found to be greater than the remained two materials, which was attributed to the densely populated chemisorbed oxygen. The authors proposed a suitable catalytic mechanism to show the generation and involvement of suitable oxygen free radicals, Ce-peroxo species and Ce(III) defects in the oxidation process.

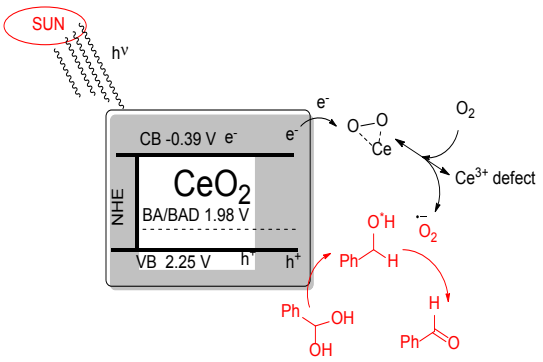

Scheme 32

According to the research work of Taniguchi *et al.,* a mesoporous ceria prepared by solvothermal method (CeO_2-AN-tEG;AN=CH_3CN, tEG = triethylene glycol) has shown improved activity than the commercially available ceria in the Bz-OL oxidation[50] (Scheme 33) using O_2 as oxidant at 60^{o}C. The Bz-AL produced in this reaction was used for the subsequent condensation with amines to form the imines. The authors developed a procedure to increase the concentration of Ce(III) ions in ceria and thereby to increase the O_2 adsorption on the catalyst surface to accelerate the selective oxidation of Bz-OL.

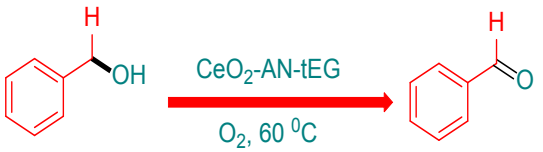

Scheme 33

Table 4: Brief details of Unsupported-Ceria catalysts promoted oxidation of Bz-OLto Bz-AL

Sr. No	Catalyst	Catalyst Synthesis	Oxidant/Solvent Bz-AL Yield/ Selectivity C/Y/S	Bz-OL Conversion/ Temperature (^{0}C)	Reaction	Reference
1	CeO_2-nano rods (110 plane)	Hydrothermal	O_2/solventless	/-/98	230	48
2	CeO_2	Hydrolyzation	O_2/MeCN, (vis. light) 400nm	100/-/100	RT	49
3	Ce^{+3} enriched mesoporous CeO_2 (crystallized from MeCN) and TEG)	Solvothermal	O_2/Toluene	-/-/90	60	50

CONCLUSION

In conclusion, this review has highlighted the effectiveness of cerium-based catalysts in optimizing the chlorine-free synthesis of Bz-AL via selective oxidation of Bz-OL using eco-friendly oxidants. By shedding light on the surface and structural attributes intrinsic to ceria-based catalysts-such as their rich oxygen vacancy content, the redox behavior of Ce(III)/Ce(IV) ions, and their acid-base properties-the review has underscored their pivotal role in facilitating selective oxidation reactions. Through a thorough examination of these catalysts' characteristics, it becomes apparent that ceria-based materials hold considerable promise as efficient and sustainable alternatives for Bz-OL oxidation. Their capacity to harness environmentally benign oxidants, coupled with their unique surface features, positions them as attractive contenders for advancing greener methodologies in Bz-AL production. Overall, this review underscores the importance of ceria-based catalysts in the quest for environmentally conscious pathways toward Bz-AL synthesis. By contributing to the development of sustainable chemistry practices, these catalysts pave the way for more eco-friendly routes in industrial processes.

ACKNOWLEDGMENT

This research did not receive any specific grant from funding agencies in the public, commercial, or not-for-profit sectors.

Conflict of Interest

There is no conflict of interest

REFERENCES

1. Satrio, J. A. B.; Doraiswamy, L. K., *Chemi. Eng. J.*, **2001**, *82*, 43-56.
2. Enache, D.I.; Edwards, J.K.; Landon, P.; Solsona-Espriu, B.; Carley, A.F.; Herzing, A.A.; Watanabe, M.; Kiely, C.J.; Knight, D.W.; Hutchings, G., *J. Science.*, **2006**, *311*, 362–365.
3. Feng, D.; Dong, Y.; Zhang, L.; Ge, X.; Zhang, W.; Dai, S.; Qiao, Z. A., *Angew. Chem. Int. Ed.*, **2020**, *59*, 19503–19509.
4. Wang, Z.; Feng, J.; Li, X.; Oh, R.; Shi, D.; Akdim, O.; Xia, M.; Zhao, L.; Huang, X.; Zhang, G., *J. Colloid Interface Sci.*, **2021**, *588*, 787–794.
5. Corey, E. J.; Fleet, G. W., *J. Tetrahedron Lett.,* **1973**, *14*, 4499-4501.
6. Javidfar, F.; Fadaeian, M.; Ghomi, J. S., *Polycycl. Aromat. Compound.*, **2022**, *42*, 5638-5648.
7. Jiang, X.; Ma, S., *Synthesis-Stuttgart.*, **2018**, *50*, 1629-1639.
8. Savara, A.; Chan-Thaw, C. E.; Rossetti, I.; Villa, A.; Prati, L., *Chem Cat Chem.*, **2014**, *6*, 3464– 3473.
9. Neto, R. C. R.; Schmal, M., *Appl. Catal. A: Gen.*, **2013**, *450*, 131-142.
10. Cam, T. S.; Omarov, S. O.; Chebanenko, M. I.; Izotova, S. G.; Popkov, V. I., *J. Sci.: Adv. Mater. Devices.*, **2022**, *7*, 100399.
11. Stoianov, O. O.; Ivanov, V. K.; Shcherbakov, A. B.; Stoyanova, I. V.; Chivireva, N. A.; Antonovich, V. P., *Russ. J. Inorg. Chem.*, **2014**, *59*, 15–23.
12. Sun, C.; Li, H.; Chen, L., *Energy Environ. Sci.*, **2012**, *5*, 8475-8505.
13. Wang, F.; Li, W.; Feng, X.; Liu, D.; Zhang, Y., *Chem. Sci.*, **2016**, *7*, 1867.
14. Sudarsanam, P.; Mallesham, B.; Durgasri D. N.; Reddy, B. M., *RSC Adv.*, **2014**, *4*, 11322-11330.
15. Tang , Y.; Zhang , H.; Cui , L.; Ouyang , C.; Shi , S.; Tang , W.; Li , H.; Lee, J. S.; Chen , L., *Phys. Rev. B: Condens. Matter Mater. Phys.*, **2010**, *82*, 125104-125112.

16. Zhen, J. M.; Liu, D. P.; Wang, X.; Li, J. Q.; Wang, F.; Wang Y. H.; Zhang, H., *J. Dalton Trans.*, **2015**, *44*, 2425-2430.
17. Zheng, H.; Wei, Z.-H.; Hu, X.-Q.; Xu, J.; Xue, B., *Chemistry Select.,* **2019**, *4*, 5470–5475.
18. Ko, W.; Kim, J.; Yim, G. H.; Lee, S. C.; Kim, S.; Kwak, M.; Choi, H.; Kim, J.; Antink, W. H.; Kim, J.; Lee, C. W.; Bok,J.; Jung, Y.; Lee, E.; Lee, K.-S.; Cho, S.-P.; Kim, D. H.; Kim, Y. G.; Lee, B.-H.; Hyeon, T.; Yoo, D., *Chem Cat Chem.*, **2022**, *14*, e202101760.
19. Zhang, L.; Chen, R.; Tu, Y.; Gong, X.; Cao, X.; Xu, Q.; Li, Y.; Ye, B.; Ye, Y.; Zhu, J., *ACS Catal.,* **2023**, *13*, 2202–2213.
20. Moeini, S. S.; Battocchio, C.; Casciardi, S.; Luisetto, I.; Lupattelli, P.; Tofani, D.; Tuti, S., *Catalysts.*, **2019**, *9*, 847.
21. Moeini, S. S.; Tuti, S.; Battocchio, C.; Luisetto, I.; Tofani, D., *Catalysts.*, **2023**, *13*, 5.
22. Wang, Z.; Zhang, B.; Yang, S.; Yang, X.; Meng, F.; Zhai,L.; Li , Z.; Zhao, S.; Zhang, G.; Qin, Y., *J. Catal.*, **2022**, *414*, 385–393.
23. Yi, X.-T.; Li, C.-Y.; Wang, F.; Xu, J.; Xue, B., *New J. Chem.*, **2022**, *46*, 7108.
24. Feng, M.; Wang, M.-Y.; Wang, F.; Xue, B.; Xu, *J. Appl. Catal. A: Gen.*, **2023**, *665*, 119384.
25. Wu, Y.; Zhang, Y.; Lv, X.; Mao, C.; Zhou, Y.; Wu, W.; Zhang , H.; Huang, Z., *J. Taiwan Inst. Chem. Eng.*, **2020**, *107*, 161-170.
26. Ketkaew, M.; Suttipat, D.; Kidkhunthod, P.; Witoon T.; Wattanakit, C., *RSC Adv.*, **2019**, *9*, 36027.
27. Hamaloglu, K. O.; Tosun, R. B.; Ulu, S.; Kay, H.; Kavakl, C.; Kip, P. A.-Ka. C.; Tuncel, A., *New J. Chem.*, **2021**, *45*, 2019.
28. Lei, L.; Liu, H.; Wu, Z.; Qin, Z.; Wang, G.; Ma, J.-Y.; Luo, L.; Fan, W.; Wang, J., *ACS Appl. Nano Mater.*, **2019**, *2*, 5214–5223.
29. Li, X.; Feng, J.; Perdjon, M.; Oh, R.; Zhao, W.; Huang, X.; Liu, S., *Appl. Surf. Sci.*, **2020**, *505*, 144473.
30. Wolski, L.; Nowaczyk, G.; Jurga, S.; Ziolek, M., *Catalysts.*, **2021**, *11*, 641.
31. García-López, E. I.; Abbasi, Z.; Parrino, F.; La Parola, V.; Liotta, L.F.; Marcì, G., *Catalysts.*, **2021**, *11*, 1467.
32. Olmos, C. M.; Chinchilla, L. E.; Villa, A.; Delgado, J. J.; Hungría, A. B.; Blanco, G.; Prati, L.; Calvino, J. J.; Chen, X., *J. Catal.*, **2019**., **375**, 44–55.
33. Dong, Y.; Luo, J.; Li, S.; Liang, C., *Catal. Commun.*, **2020**, *133*, 105843.
34. Gu, J.; Liu, H.; Peng, T.; Li, S.; Xu, L.; Zhang, J.; Zhang, L., *ACS Appl. Nano Mater.*, **2022**, *5*, 4972–4982.
35. Keshri, K. S.; Spezzati, G.; Ruidas, S.; Hensen, E. J. M.; Chowdhury, B., *Catal. Commun.*, **2020**, *140*, 106004.
36. Aneggi, E.; Campagnolo, F.; Segato, J.; Zuccaccia, D.; Baratta , W.; Llorca, J.; Trovarelli, A., *Mol. Catal.,* **2023**, *540*, 113049.
37. Laga, S. M.; Townsend, T. M.;O'Connor, A. R.; Mayer, J. M., *Inorg. Chem. Front.*, **2020**, *7*, 1386-1393.
38. Diez, A. S.; Piqueras, C. M.; Araiza, D. G.; Díaz, G.; Volpe, M. A., *Mater. Chem. Phys.*, **2019**, *232*, 265-271.
39. Pischetola, Ch.; Francis, S. M.; Grillo, F.; Baddeley, C. J.; Lizana, F. C., *J. Catal.,* **2021**, *394*, 316-331.
40. Challa, P.; Enumula, S. S.; Reddy, K. S.; Kondeboina, M.; Burri, D. R.; Kamaraju, S. R. R., *Ind. Eng. Chem. Res.*, **2020**, *59*, 17720–17728.
41. Hao, J.; Long, Z.; Sun, L.; Zhan, W.; Wang, X.; Han, X., *Inorg. Chem.*, **2021**, *60*, 7732–7737.
42. Priya, A. S.; Devi, K R S.; Venkatesha, N. J., *J. Aust. Ceram. Soc.*, **2020**, *56*, 217-225.
43. Mazumder, T.; Dandapat, S.; Baidya, T.; Likhar, P. R.; Clark,A. H.;Bera, P.; Tiwari, K.; Payra, S.; Rao, B. S.; Roy,S.; Biswas, K.J., *Phys. Chem. C.*, **2021**, *125*, 20831-20844.
44. Turgut, A. M.; Ozer, D.; Icten, O.; Zumreoglu-Karan, B., *Catal. Lett.*, **2023**, *153*, 1719–1725.
45. Xu , C.; Zhong , S.; Yuan , L.; Yu , M.; Chen, Y.; Dai, L.; Wang, X., *Chem Eng J.*, **2024**, *481*, 148767.
46. Aiube C. M.; de Macedo, J. L., *Microporous and Mesoporous Mater.*, **2022**, *346*, 112326.
47. Akinnawo, C. A.; Bingwa, N.; Meijboom, R., *Catal. Commun.*, **2020**, *45*, 106115.
48. Zhou, Q.; Zhou, C.; Zhou, Y.; Hong, W.; Zou, S.; Gong, X.-Q.; Liu, J.; Xiao, L.; Fan, *J. Catal. Sci. Technol.*, **2019**, *9*, 2960-2967.
49. Cui, Z.; Zhou, H.; Wang, G.; Zhang, Y.; Zhang, H.; Zhao, H., *New J. Chem.*, **2019**, *43*, 7355-7362.
50. Taniguchi, A.; Kumabe, Y.; Kan, K.; Ohtani, M.; Kobiro, K., *RSC Adv.,* **2021**, *11*, 5609-5617.